

# We are IntechOpen, the world's leading publisher of Open Access books Built by scientists, for scientists

4,800

Open access books available

122,000

International authors and editors

135M

Downloads

Our authors are among the

154

Countries delivered to

TOP 1%

most cited scientists

12.2%

Contributors from top 500 universities



WEB OF SCIENCE™

Selection of our books indexed in the Book Citation Index  
in Web of Science™ Core Collection (BKCI)

Interested in publishing with us?  
Contact [book.department@intechopen.com](mailto:book.department@intechopen.com)

Numbers displayed above are based on latest data collected.  
For more information visit [www.intechopen.com](http://www.intechopen.com)



---

# Finite Element Modelling of the Dynamic Behaviour of Tubular Footbridges

---

José Guilherme Santos da Silva, Ana Cristina Castro Fontenla Sieira, Gilvan Lunz Debona, Pedro Colmar Gonçalves da Silva Vellasco and Luciano Rodrigues Ornelas de Lima

Additional information is available at the end of the chapter

<http://dx.doi.org/10.5772/50376>

---

## 1. Introduction

Tubular hollow sections are increasingly used in off-shore structures, highway bridges, pedestrian foot-bridges, large-span roofs and multi-storey buildings due to their excellent properties and the associated advances in fabrication technology. The intensive use of tubular structural elements in Brazil, such as the example depicted in Figure 1, mainly due to its associated aesthetical and structural advantages, led designers to be focused on their technologic and design issues.

Nowadays in Brazil, there is still a lack of code that deals specifically with tubular design. This fact induces designers to use other international tubular design codes. Consequently, their design methods accuracy plays a fundamental role when economical and safety points of view are considered. Additionally, recent tubular joint studies indicate that further research is needed, especially for particular geometries. This is even more significant for some failure modes where the collapse load predictions lead to unsafe or uneconomical solutions.

Steel and composite tubular footbridges are currently subjected to dynamic actions with variable magnitudes due to the pedestrian crossing on the concrete deck [1-4]. These dynamic actions can generate the initiation of fractures or even their propagation in the structure. Depending on the magnitude and intensity, these adverse effects can compromise the structural system response and the reliability which may also lead to a reduction of the expected footbridge service life.

Generally, fatigue assessment procedures are usually based on S-N curves which relate a nominal or geometric stress range  $S$  to the corresponding number  $N$  of load cycles to fatigue

failure. In this situation fatigue assessment refers to the nominal stress range  $\Delta\sigma$  in a tubular structural member.



**Figure 1.** Example of a tubular steel pedestrian footbridge in Rio de Janeiro/RJ, Brazil.

The fatigue resistance is given according to a classification catalogue in the form of standardized S-N curves. Structural details classified in this catalogue, see e.g. Eurocode 3 Part 1.9 [5], correspond specifically to a situation of stress range, direction, crack position, detail dimension and weld quality which had been characteristic for the tests on which the classification is based [6-7].

The use of circular hollow section members as part of the structure of pedestrian footbridges is a relatively new constructional concept. During the last couple years several steel-concrete composite footbridges had been constructed in Brazil, as illustrated in Figure 1.

The typical cross-section of this type of pedestrian footbridge generally consists of a tubular spatial truss girder carrying the concrete deck slab, as presented in Figure 1. The deck slab is connected directly to the steel structure by either shear studs, concrete dowels or in some cases where no top chord exists. At the bottom chord of the tubular space truss four brace members have to be connected to the continuous bottom chord. This type of joint is usually named K-joint, as depicted in Figure 2 [6].

Steel and composite tubular footbridges can be subjected to the material imperfections of its structural elements, such as mechanical and metallurgic discontinuities. Such defects lead to cracking in these structural elements. When these elements are subjected to dynamic actions, the fatigue phenomenon occurs and produces stress concentrations and possible fractures. These fractures are directly responsible for reducing the local or global footbridge stabilities or even its life service [7].

On the other hand, the structural engineers experience and knowledge allied by the use newly developed materials and technologies have produced tubular steel and composite (steel-concrete) footbridges with daring structures. This fact have generated very slender tubular steel and composite pedestrian footbridges and consequently changed the serviceability and ultimate limit states associated to their design. A direct consequence of this design trend is a considerable increase of structural vibrations [1-4, 8-11].

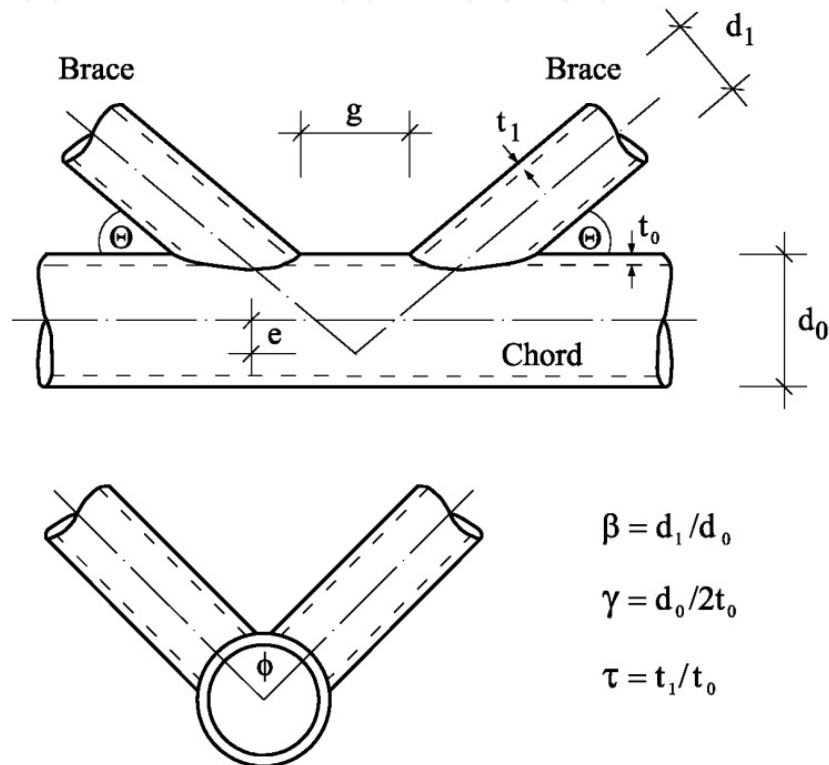


**Figure 2.** Typical multiplanar K-joint with notations.

Considering all aspects mentioned before, the main objective of this investigation is to present the finite element modelling of the dynamic behaviour of tubular composite (steel-concrete) footbridges submitted to human walking vibration. Based on the results obtained in this study, a fatigue assessment will be performed, in order to evaluate the tubular footbridges service life. Further research in this area is currently being carried out.

The investigated structural model was based on a tubular composite (steel-concrete) footbridge, spanning 82.5 m. The structure is composed by three spans (32.5 m, 17.5 m and 20.0 m, respectively) and two overhangs (7.50 m and 5.0 m, respectively). The structural system consists of tubular steel sections and a concrete slab and is currently used for pedestrian crossing [1-2].

The proposed computational model adopted the usual mesh refinement techniques present in finite element method simulations, based on the ANSYS program [13]. The finite element model has been developed and validated with the experimental results. This numerical model enabled a complete dynamic evaluation of the investigated tubular footbridge especially in terms of human comfort and its associated vibration serviceability limit states.

This investigation is carried out based on correlations between the experimental results related to the footbridge dynamic response and those obtained with finite element models [1-2]. The structural system dynamic response, in terms of peak accelerations, was obtained and compared to the limiting values proposed by several authors and design standards [9,14].

The peak acceleration values found in the present investigation indicated that the analysed tubular footbridge presented problems related with human comfort. Hence it was detected that this type of structure can reach high vibration levels that can compromise the footbridge user's comfort and especially its safety.

## 2. Human walking modelling

Human loads comprise a large portion of the acting live loads in offices and residential building floors. In general, the human live loads are classified into two broad categories: in situ and moving. Periodic jumping due to music, sudden standing of a crowd, and random in-place movements are examples of in situ activities. Walking, marching, and running are examples of moving activities. As the main purpose of footbridges is the pedestrian's crossing, they must be safe and do not cause discomfort to users [1-4].

On the other hand, human activities produce dynamic forces and their associate vibration levels should not disturb or alarm their users. Therefore, this investigation describes four different load models developed to incorporate the dynamic effects induced by people walking on the footbridges dynamic response. It must be emphasized that the geometry of the human body walking is an organized leg motion that cause an ascent and descending movement of the effective body mass at each step [1-4].

The human body mass accelerations are associated to floor reactions, and are approximately periodic to the step frequency. The two feet produce this type of load, as function of the static parcel associated to the individual weight and three or four harmonic load components. These harmonics appear due to the interaction between the increasing loads, represented by one foot, and the simultaneous unload of the other foot [1-4].

However, it is also necessary to incorporate several other parameters in the human walking representation, like step distance and speed. These variables are related to the step frequency and are depicted in Table 1 [12]. Table 1 presents a detailed description of the excitation frequency values, dynamic coefficients, as well as the phase angles to be employed in the mathematical representation of the four dynamic loading models implemented and used in the present investigation.

Activity	Velocity (m/s)	Step Distance (m)	Step Frequency (Hz)
Slow Walking	1.1	0.60	1.7
Normal Walking	1.5	0.75	2.0
Fast Walking	2.2	1.00	2.3

**Table 1.** Characteristics of the human walking [12].

## 2.1. Load model I (LM-I)

This walking load model can be represented by the load static parcel, related to the individual weight, and a combination of harmonic forces whose frequencies are multiples or harmonics of the basic frequency of the force repetition, e.g. step frequency,  $f_s$ , for human activities. This load model considers a space and temporal variation of the dynamic action over the structure and the time-dependent repeated force can be represented by the Fourier series, see Equation (1).

$$F(t) = P[1 + \sum \alpha_i \cos(2\pi i f_s t + \phi_i)] \quad (1)$$

Where:

- $F(t)$  : dynamic load;
- $P$  : person's weight (800 N [1-4]);
- $\alpha_i$  : dynamic coefficient for the harmonic force;
- $i$  : harmonic multiple ( $i = 1, 2, 3, \dots, n$ );
- $f_s$  : walking step frequency;
- $\phi$  : harmonic phase angle;
- $t$  : time.

In this load model, five harmonics were considered to represent the dynamic load associated to human walking [12]. Table 2 shows the dynamic coefficients and phase angles used in this load model. Figure 3 presents a dynamic loading function for one person walking with step frequency equal to 2 Hz.

Harmonic $i$	Dynamic Coefficients $\alpha_i$	Phase Angles $\phi_i$
1	0.37	0
2	0.10	$\pi/2$
3	0.12	$\pi/2$
4	0.04	$\pi/2$
5	0.08	$\pi/2$

**Table 2.** Dynamic coefficients and phase angles [12].

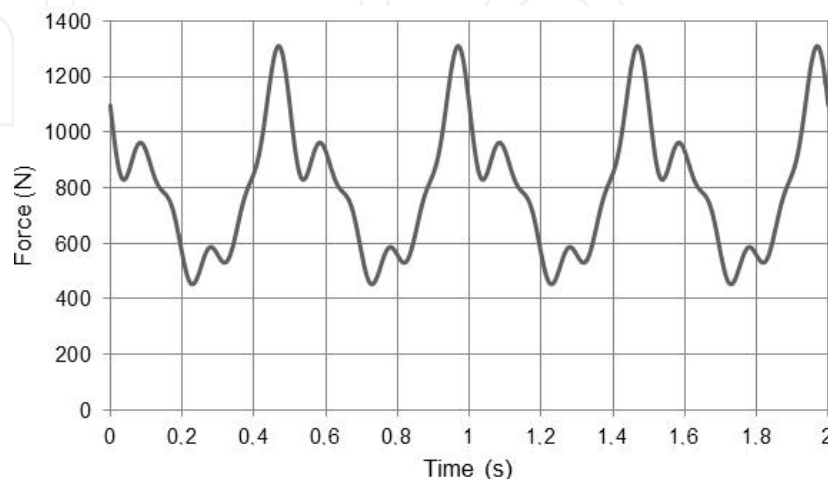


**Figure 3.** LM-I: dynamic load function for one person walking ( $f_s = 2.0$  Hz).

## 2.2. Load model II (LM-II)

In this load model, the time-dependent repeated force also can be represented by the Fourier series, as expressed in Equation (1) and four harmonics were considered to represent the dynamic action associated to human walking [9]. This model also considers a space and temporal variation of the dynamic action over the structural system. Table 3 shows the dynamic coefficients and phase angles used in this model. Figure 4 presents a dynamic loading function for one person walking with step frequency equal to 2 Hz.

Harmonic $i$	Dynamic Coefficients $\alpha_i$	Phase Angles $\phi_i$
1	0.50	0
2	0.20	$\pi/2$
3	0.10	$\pi$
4	0.05	$3\pi/2$

**Table 3.** Dynamic coefficients and phase angles [9].

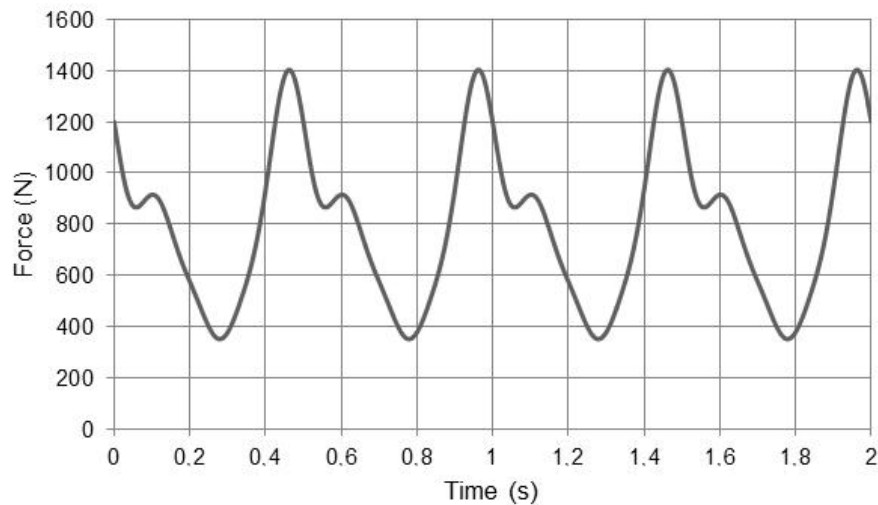


**Figure 4.** LM-II: dynamic load function for one person walking ( $f_s = 2.0$  Hz).

## 2.3. Load model III (LM-III)

In this case a general expression is used to represent the excitation produced by an individual walking throughout time. These loads are produced with both feet, as function of a static part associated to the individual weight and three harmonics were considered to represent the dynamic action related to human walking [15], as illustrated in Equation (2). This dynamic loading model considers a space and temporal variation of the dynamic action over the footbridge.

$$F(t) = P + \Delta P_1 \sin(2\pi f_s t - \phi_1) + \Delta P_2 \sin(4\pi f_s t - \phi_2) + \Delta P_3 \sin(6\pi f_s t - \phi_3) \quad (2)$$

Where:

- $F(t)$  : dynamic load;
- $P$  : person's weight (800 [1-4]);
- $f_s$  : walking step frequency;

$\phi_i$  : harmonic phase angle;  
 $t$  : time.

In Equation (2), the magnitudes  $\Delta P_1$ ,  $\Delta P_2$  and  $\Delta P_3$  are associated with harmonic amplitudes. The first harmonic amplitude,  $\Delta P_1$ , is equal to  $0.4P$  for  $f_s$  equal to 2.0 Hz and  $0.5P$  for  $f_s$  equal to 2.4Hz. A simple interpolation between these two values can be used in intermediate cases. The second and third harmonic amplitudes,  $\Delta P_2$  e  $\Delta P_3$ , were assumed to be equal to  $0.1P$  for  $f_s$  equal to 2.0Hz [15].

The phase angles  $\phi_2$  and  $\phi_3$  depend on various other factors and should represent the most favourable used load combinations. In the present study the phase angles  $\phi_2$  and  $\phi_3$  were assumed to be equal to  $\pi/2$  and phase angle  $\phi_1$  was assumed to be equal to zero [15]. Figure 5 presents a dynamic loading function for one person walking with step frequency equal to 2 Hz.

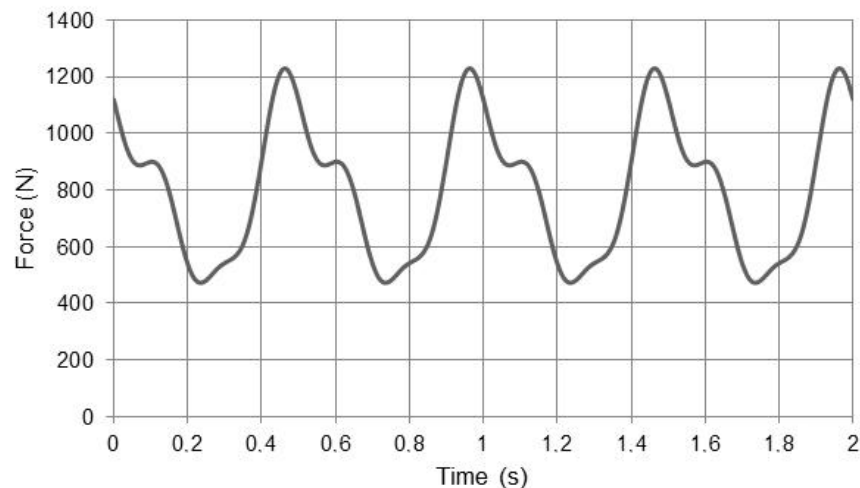


**Figure 5.** LM-III: dynamic load function for one person walking ( $f_s = 2.0$  Hz).

#### 2.4. Load model IV (LM-IV)

The fourth walking load model considered the same idea of the previous models. The main difference was the incorporation of the human heel effect in this particular load representation with the aid of Equations (3) to (6). The mathematical model behind this strategy was proposed by Varela [8] as well as a numerical approach to evaluate the floor structure reaction, as presented in Figure 6.

The proposed mathematical model, see Equations (3) to (6), used to represent the dynamic actions produced by people walking on floor slabs is not simply a Fourier series. This is due to the fact that the mentioned equations also incorporate the heel impact effect [8]. This loading model also considers a space and temporal variation of the dynamic action over the structure and is evaluated considering four harmonics.

Additionally, Load Model IV (LM-IV) also incorporates the transient effect due to the human heel impact [8]. The present investigation used a heel impact factor equal to 1.12 ( $f_{mi}$



= 1.12). However, it must be emphasized that this value can vary substantially from person-to-person. Figure 6 illustrates the dynamical load function for an individual walking at 2 Hz, based on Equations (3) to (6) and Tables 1 and 3 [9,12].

### 3. Investigated structural model

The structural model consists of tubular steel sections and a 100 mm concrete slab and is currently submitted to human walking loads [1-2]. The structure was based on a tubular composite (steel-concrete) footbridge, spanning 82.5 m. The structure is composed by three spans (32.5 m, 17.5 m and 20.0 m, respectively) and two overhangs (7.50 m and 5.0 m, respectively), as illustrated in Figures 7 and 8.

The steel sections used were welded wide flanges (WWF) made with a 300 MPa yield stress steel grade. A Young's modulus equal to  $2.05 \times 10^5$  MPa was adopted for the tubular footbridge steel beams and columns. The concrete slab has a 20 MPa specified compression strength and a  $2.13 \times 10^4$  MPa Young's Modulus.

$$F(t) = \begin{cases} \left( \frac{f_{mi} F_m - P}{0.04 T_p} \right) t + P & \text{if } 0 \leq t < 0.04 T_p \\ f_{mi} F_m \left[ \frac{C_1 (t - 0.04 T_p)}{0.02 T_p} + 1 \right] & \text{if } 0.04 T_p \leq t < 0.06 T_p \\ F_m & \text{if } 0.06 T_p \leq t < 0.15 T_p \\ P + \sum_{i=1}^{nh} P \alpha \text{sen} \left[ 2\pi f_p (t + 0.1 T_p) + \phi_i \right] & \text{if } 0.15 T_p \leq t < 0.90 T_p \\ 10(P - C_2) \left( \frac{t}{T_p} - 1 \right) + P & \text{if } 0.90 T_p \leq t < T_p \end{cases} \quad (3)$$

$$F_m = P \left( 1 + \sum_{i=1}^{nh} \alpha_i \right) \quad (4)$$

$$C_1 = \left( \frac{1}{f_{mi}} - 1 \right) \quad (5)$$

$$C_2 = \begin{cases} P(1 - \alpha_2) & \text{if } nh = 3 \\ P(1 - \alpha_2 + \alpha_4) & \text{if } nh = 4 \end{cases} \quad (6)$$

Where:

- $F_m$  : maximum Fourier series value, given by Equation (4);  
 $f_{mi}$  : human heel impact factor;  
 $T_p$  : step period;  
 $f_s$  : step frequency;  
 $\phi_i$  : harmonic phase angle;  
 $P$  : person's weight;  
 $\alpha_i$  : dynamic coefficient for the harmonic force;  
 $i$  : harmonic multiple ( $i = 1, 2, 3, \dots, n$ );  
 $t$  : time;  
 $C1, C2$  : coefficients given by Equations (5) and (6).

#### 4. Finite element model

The developed computational model adopted the usual mesh refinement techniques present in finite element method simulations, based on the ANSYS program [13]. The finite element model has been developed and validated with the experimental results [1-2]. This numerical model enabled a complete dynamic evaluation of the investigated tubular footbridge especially in terms of human comfort and its associated vibration serviceability limit states, see Figure 9. In this model, all steel tubular sections were represented by three-dimensional beam elements (PIPE16 and BEAM44) with tension, compression, torsion and bending capabilities. These elements have six degrees of freedom at each node: translations in the nodal  $x$ ,  $y$ , and  $z$  directions and rotations about  $x$ ,  $y$ , and  $z$  axes, see Figure 9.

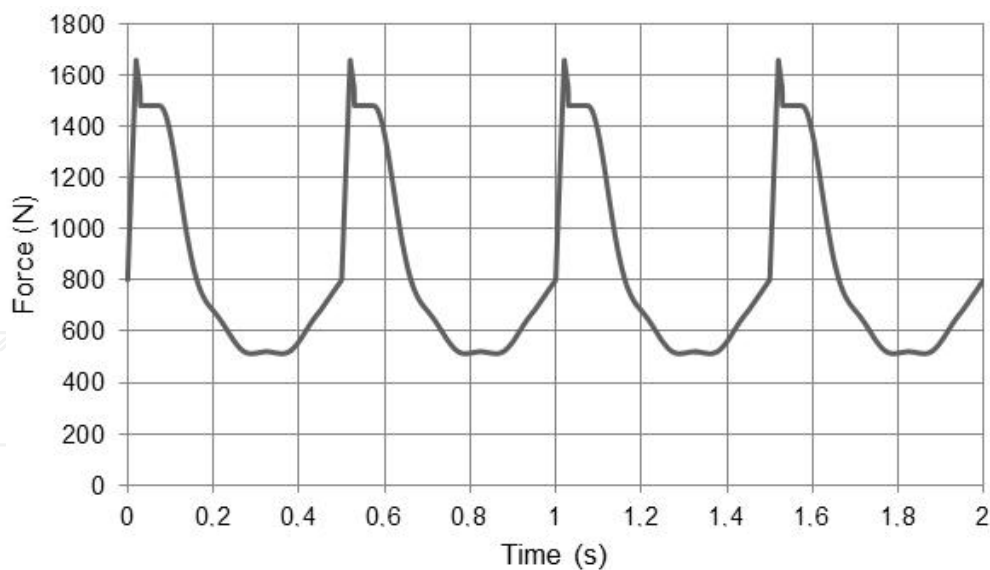


**Figure 6.** LM-IV: dynamic load function for one person walking ( $f_p = 2.0$  Hz).

On the other hand, the reinforced concrete slab was represented by shell finite elements (SHELL63), as presented in Figure 9. This finite element has both bending and membrane capabilities. Both in-plane and normal loads are permitted. The element has six degrees of freedom at each node: translations in the nodal  $x$ ,  $y$ , and  $z$  directions and rotations about the nodal  $x$ ,  $y$ , and  $z$  axes.



**Figure 7.** Investigated steel-concrete composite tubular footbridge.



**Figure 8.** Internal section of the investigated structural model.

The footbridge pier bearings were represented by a non-linear rotational spring element (COMBIN39). This element is a unidirectional element with non-linear generalized force-deflection capability that can be used in any analysis.

The finite element model presented 71540 degrees of freedom, 11938 nodes and 15280 finite elements (BEAM44: 1056; PIPE16: 5642; SHELL63: 8580 and COMBIN39: 8), as presented in Figure 9. It was considered that both structural elements (steel tubular sections and concrete slab) have total interaction with an elastic behaviour.

## 5. Dynamic analysis

Initially, the steel-concrete composite tubular footbridge natural frequencies, vibration modes and peak accelerations were determined based on experimental tests [2]. The peak acceleration values were obtained considering three types of human walking: slow walking, regular walking and fast walking.

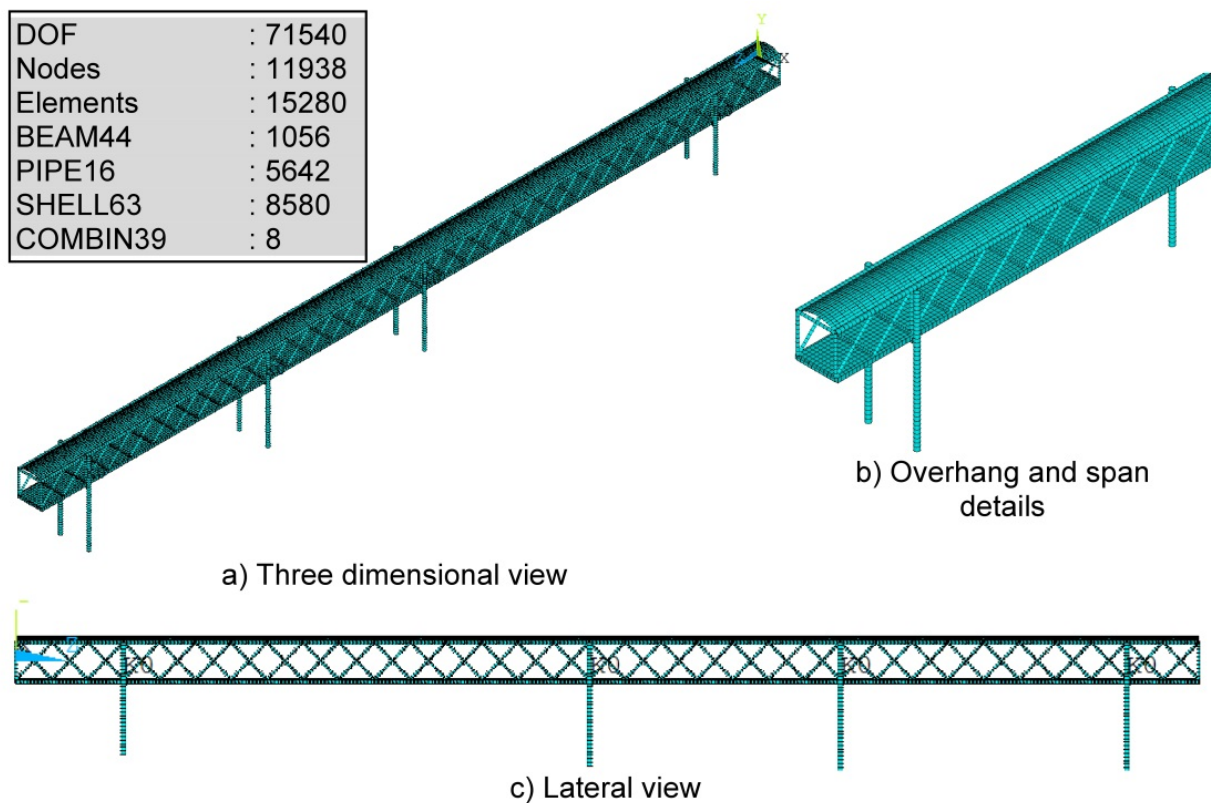


**Figure 9.** Tubular footbridge finite element model

In a second phase, the steel-concrete composite tubular footbridge natural frequencies vibration modes and peak accelerations were determined with the aid of the numerical simulations [1], based on the finite element method using the ANSYS program [13].

### 5.1. Natural frequencies and vibration modes

It can be clearly noticed that there is a very good agreement between the structural model natural frequency values calculated using finite element simulations [1] and the experimental results [2], see Table 4. Such fact validates the finite element model here presented, as well as the results and conclusions obtained throughout this investigation. The vibration modes of the tubular footbridge are depicted in Figures 10 to 12.

Tubular Footbridge Natural Frequencies (Hz)	$f_{01}$	$f_{02}$	$f_{03}$
Finite Element Model (see Figure 9)	1.61	2.12	5.39
Experimental Results	1.56	2.34	5.08
Error (%)	3.20	9.40	6.10

**Table 4.** Tubular footbridge natural frequencies.

When the tubular footbridge freely vibrates in a particular mode, it moves up and down with a certain configuration or mode shape. Each footbridge natural frequency has an

associated mode shape. It was verified that longitudinal amplitudes were predominant in the fundamental vibration mode ( $f_{01} = 1.61$  Hz), related with Z axis direction, see Figure 10. In the second mode shape lateral displacements were predominant ( $f_{02} = 2.12$  Hz), associated with X axis direction, as presented in Figure 11. On the other hand, in the third vibration mode ( $f_{03} = 5.39$  Hz), the flexural effects were predominant, related to vertical amplitudes in the Y axis direction, as illustrated in Figure 12.

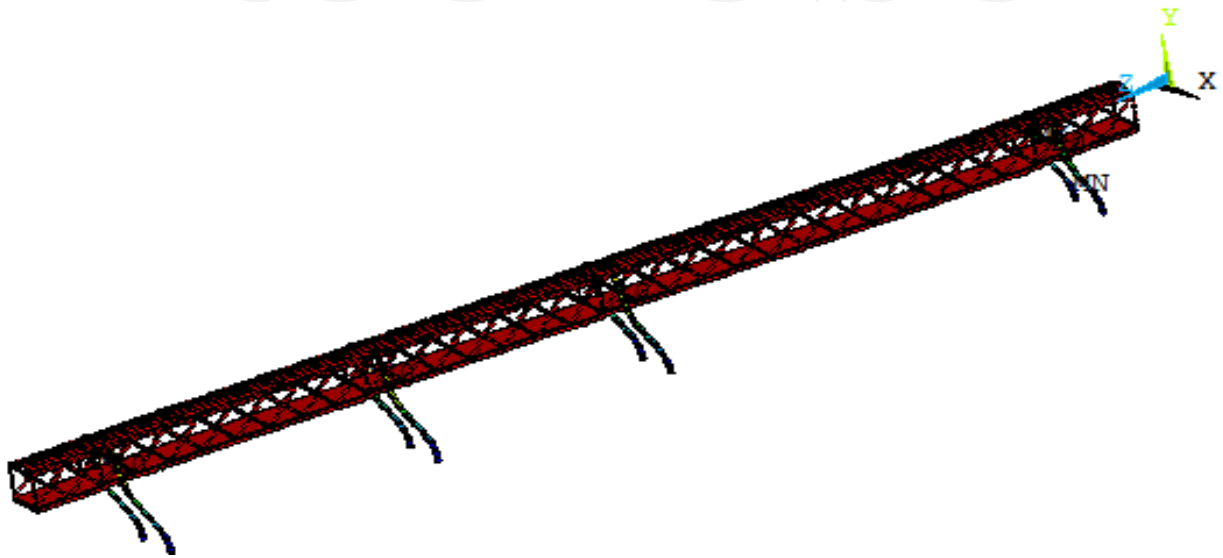


**Figure 10.** Vibration mode associated with the 1<sup>st</sup> footbridge natural frequency ( $f_{01}=1.61$  Hz).

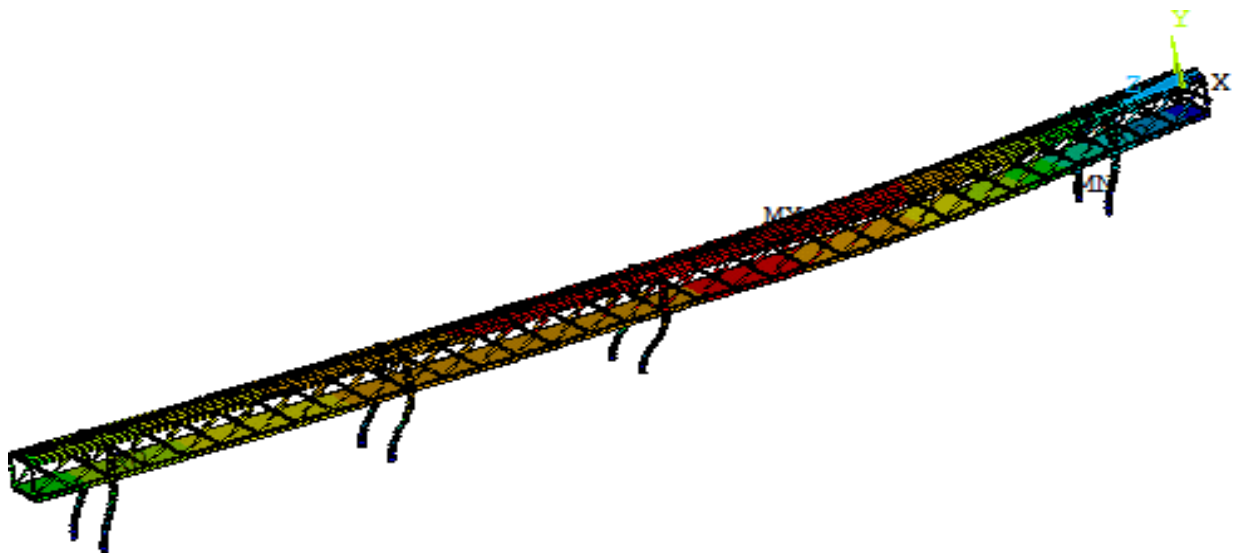


**Figure 11.** Vibration mode associated with the 2<sup>nd</sup> footbridge natural frequency ( $f_{02}=2.12$  Hz).

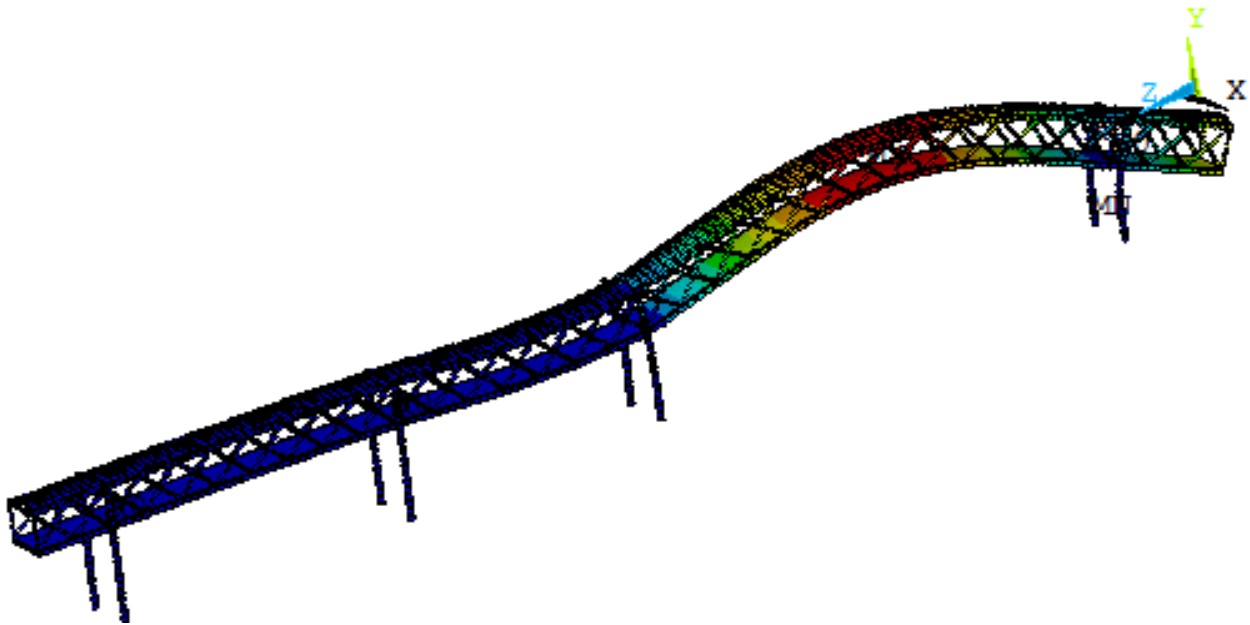


**Figure 12.** Vibration mode associated with the 3<sup>rd</sup> footbridge natural frequency ( $f_{03}=5.39\text{Hz}$ ).

## 5.2. Determination of the tubular footbridge peak accelerations

The finite element modelling follows with the evaluation of the footbridge performance in terms of vibration serviceability due to dynamic forces induced by people walking. The first step of this investigation concerned in the determination of the tubular footbridge peak accelerations, based on a linear time-domain dynamic analysis.

The dynamic loading models (see Equations (1) to (6) and Figures 3 to 6), related to one, two and three people crossing the tubular footbridge on the concrete slab centre, in normal walking, see Figures 13 to 15, were applied on the investigated footbridge over 55.0 s.

The maximum accelerations (peak accelerations) were obtained utilizing an integration time step of  $2 \times 10^{-3}$  s ( $\Delta t = 2 \times 10^{-3}$  s). In this investigation, seven sections of the structural model were analysed, see Figure 16. These maximum accelerations were compared to the limits recommended by design codes [9,14]. The structural damping coefficient adopted in this investigation was equal to 0.01 ( $\zeta=1\%$ ), in accordance with the measured experimental damping [2].

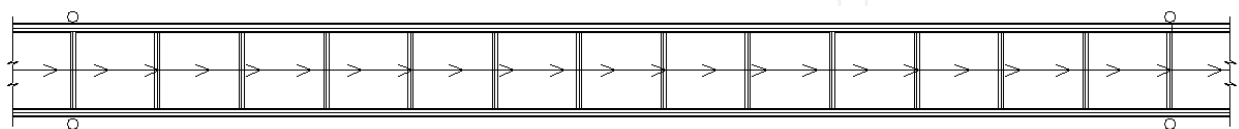


**Figure 13.** One person walking on the footbridge (regular walking).

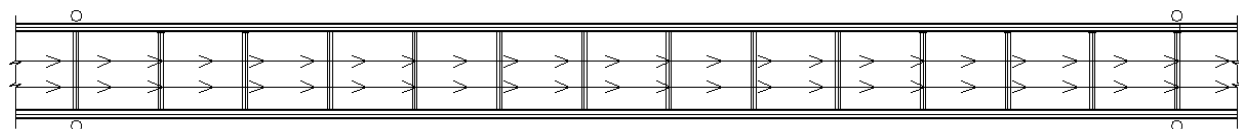


**Figure 14.** Two people walking on the footbridge (regular walking).

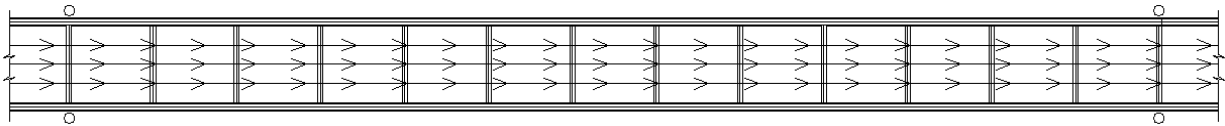


**Figure 15.** Three people walking on the footbridge (regular walking).

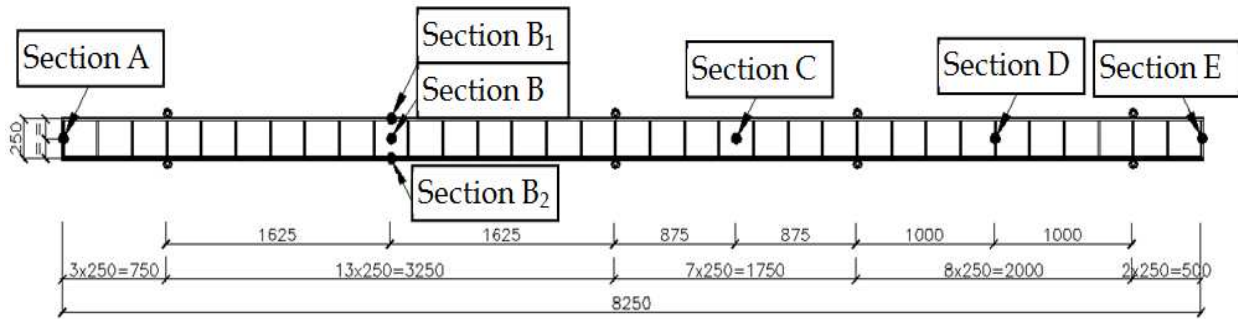


**Figure 16.** Tubular composite (steel-concrete) footbridge investigated sections.

In sequence, Figures 17 to 20 illustrate the tubular footbridge dynamic response, along the time, related to the section B (see Figure 16), when one pedestrian crosses the footbridge in regular walking (resonance condition).

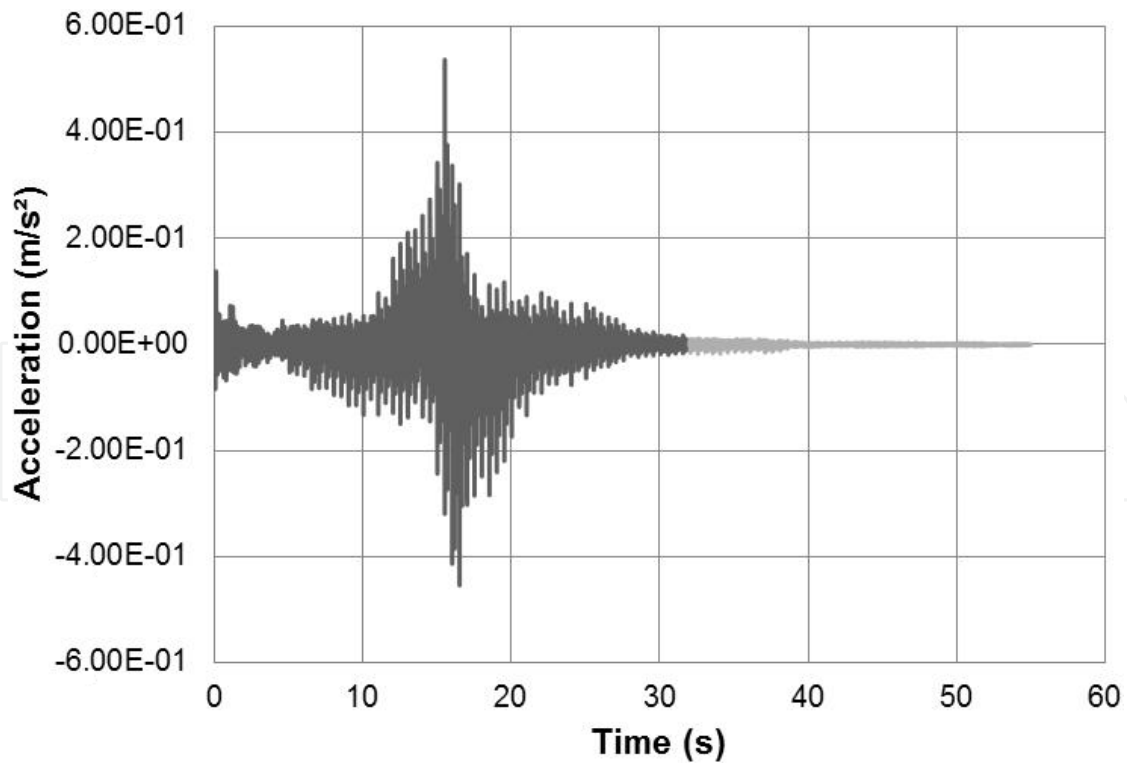


**Figure 17.** LM-I: tubular footbridge acceleration response at section B. One pedestrian crossing the concrete slab centre at resonance condition. Normal walking.

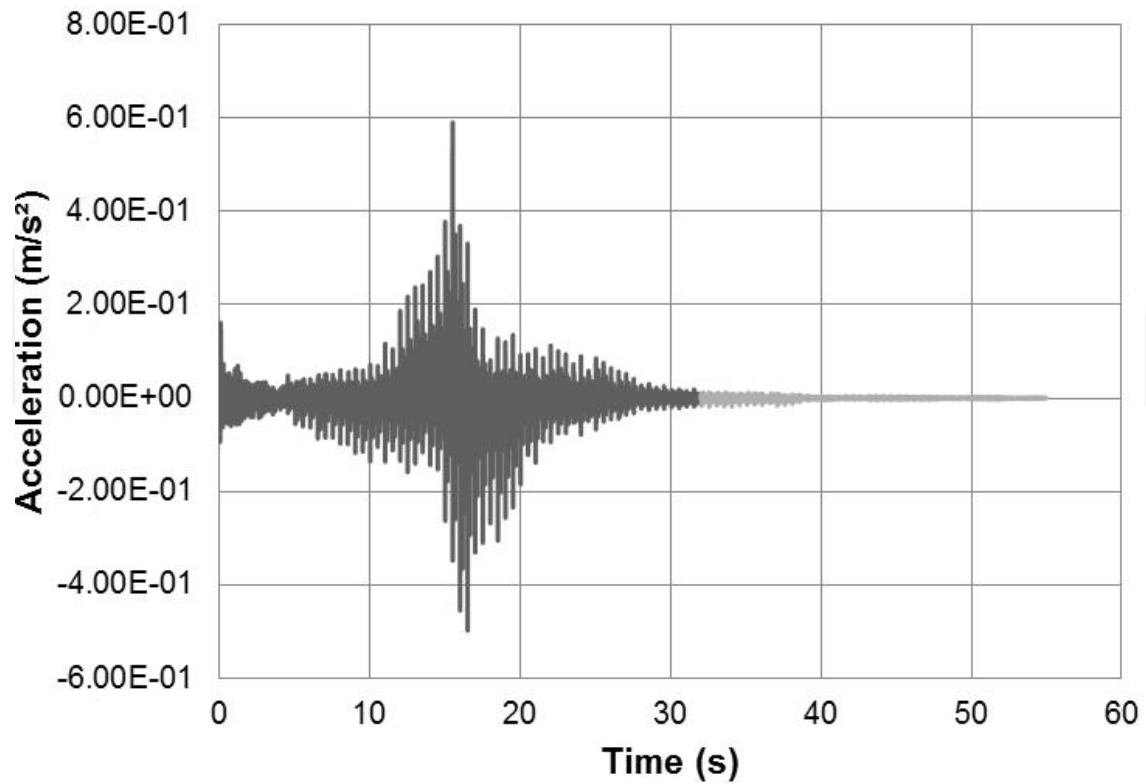


**Figure 18.** LM-II: tubular footbridge acceleration response at section B. One pedestrian crossing the concrete slab centre at resonance condition. Normal walking.

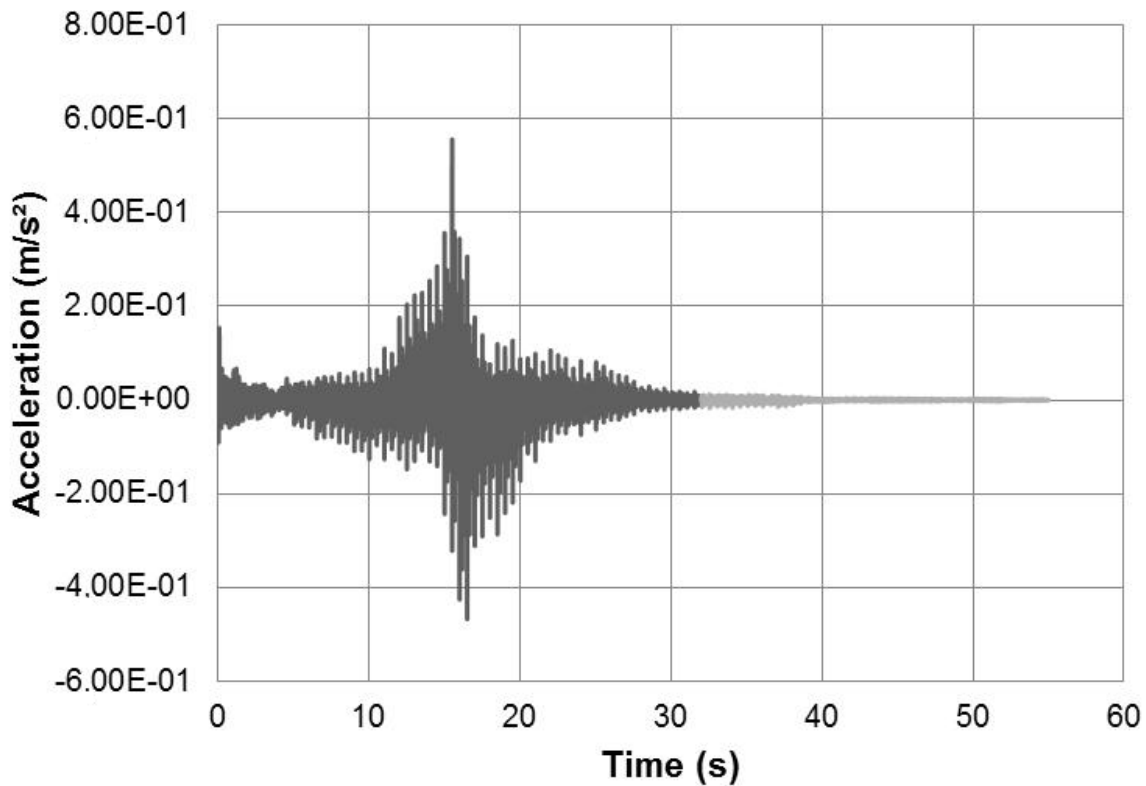


**Figure 19.** LM-III: tubular footbridge acceleration response at section B. One pedestrian crossing the concrete slab centre at resonance condition. Normal walking.



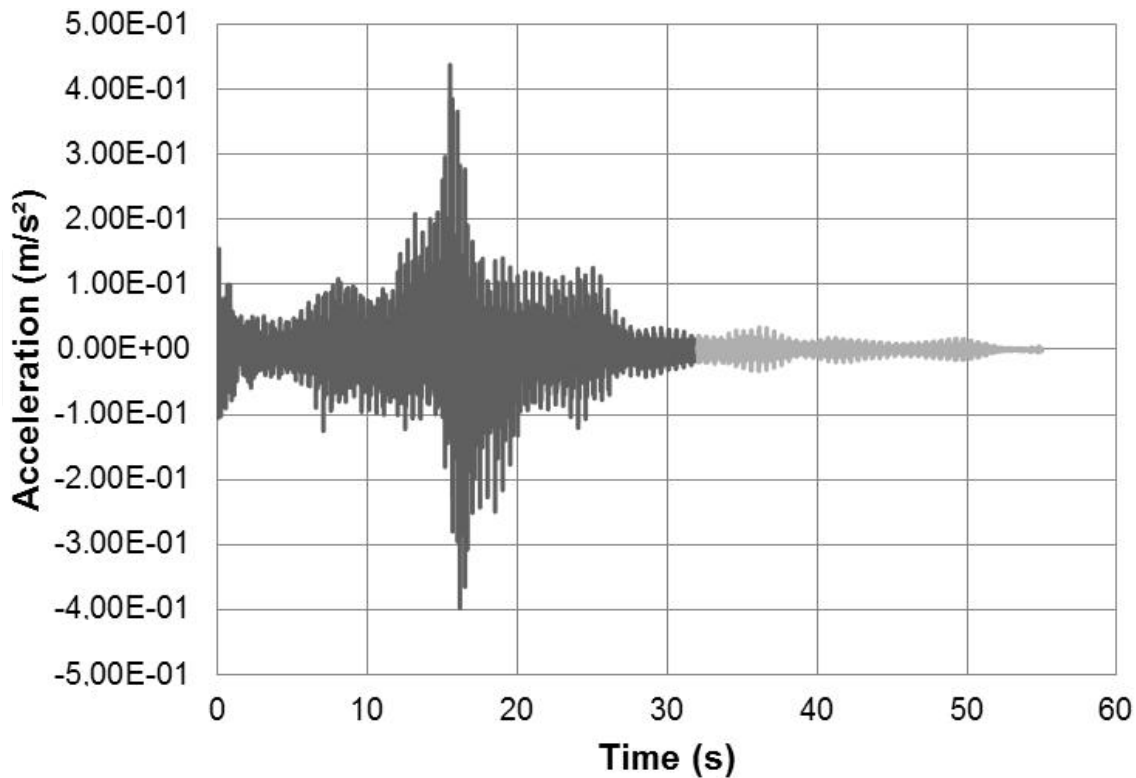


**Figure 20.** LM-IV: tubular footbridge acceleration response at section B. One pedestrian crossing the concrete slab centre at resonance condition. Normal walking.

Figures 17 to 20 present the vertical acceleration versus time graph for the tubular footbridge at section B (see Figure 16). These figures show that the vertical acceleration of the structure gradually increase along the time. In this particular case, the third harmonic with a 2.0 Hz step frequency ( $f_s = 2.0$  Hz), was the walking load resonant harmonic.

The maximum acceleration value found at section B (see Figure 16) was equal to  $0.53 \text{ m/s}^2$  (LM-I),  $0.58 \text{ m/s}^2$  (LM-II),  $0.55 \text{ m/s}^2$  (LM-III) and  $0.44 \text{ m/s}^2$  (LM-IV), as illustrated in Figures 17 to 20. These figures also indicate that from the moment that the pedestrian leaves the footbridge span (Section B, see Figure 16), when the time is approximately equal to 26 s, the structural damping minimises the dynamic structural model response, as presented in Figures 17 to 20. This assertive occurs only in dynamic loading models that consider the load spatial variation.

The peak acceleration analysis was focused on the steel-concrete composite tubular footbridge dynamic behaviour when the pedestrian normal walking was considered in this work. In sequence, Tables 5 to 7 present the maximum accelerations (peak accelerations:  $a_p$  in  $\text{m/s}^2$ ), related to seven structural sections of the investigated footbridge (A, B, B1, B2, C, D and E), as illustrated in Figure 16.

The maximum acceleration values (peak accelerations) found in this investigation are respectively equal to  $1.50 \text{ m/s}^2$  (Section A),  $0.18 \text{ m/s}^2$  (Section B1),  $0.58 \text{ m/s}^2$  (Section B),  $0.18 \text{ m/s}^2$  (Section B2),  $0.58 \text{ m/s}^2$  (Section C),  $0.43 \text{ m/s}^2$  (Section D) and  $0.79 \text{ m/s}^2$  (Section C), corresponding to one individual crossing the composite footbridge in normal walking (resonance condition), as illustrated in Figure 13.

On the other hand, these maximum acceleration values increases when the normal walking associated to two and three people (see Figures 14 and 15) is considered in the analysis, as presented in Tables 5 to 7.

Dynamic Loading Models	Tubular Footbridge Peak Accelerations ( $a_p$ in $m/s^2$ )							Limit Accelerations ( $a_{lim}$ in $m/s^2$ )*
	Investigated Sections							
	A	B <sub>1</sub>	B	B <sub>2</sub>	C	D	E	
Load Model I (LM-I)	1.38	0.17	0.53	0.17	0.53	0.39	0.72	0.49
Load Model I (LM-II)	1.50	0.18	0.58	0.18	0.58	0.43	0.79	
Load Model I (LM-III)	1.38	0.17	0.55	0.17	0.55	0.40	0.74	
Load Model I (LM-IV)	1.00	0.16	0.44	0.16	0.38	0.33	0.78	

\* $a_{lim} = 1.5\%g = 0.15 m/s^2$ : indoor footbridges [9,14]

\* $a_{lim} = 5.0\%g = 0.49 m/s^2$ : outdoor footbridges [9,14]

**Table 5.** Structural model peak accelerations corresponding to one individual walking.

Dynamic Loading Models	Tubular Footbridge Peak Accelerations ( $a_p$ in $m/s^2$ )							Limit Accelerations ( $a_{lim}$ in $m/s^2$ )*
	Investigated Sections							
	A	B <sub>1</sub>	B	B <sub>2</sub>	C	D	E	
Load Model I (LM-I)	2.14	0.19	0.74	0.19	0.72	0.61	1.23	0.49
Load Model I (LM-II)	2.32	0.21	0.81	0.21	0.80	0.67	1.35	
Load Model I (LM-III)	2.14	0.20	0.76	0.19	0.75	0.63	1.27	
Load Model I (LM-IV)	1.87	0.21	0.57	0.22	0.58	0.55	1.36	

\* $a_{lim} = 1.5\%g = 0.15 m/s^2$ : indoor footbridges [9,14]

\* $a_{lim} = 5.0\%g = 0.49 m/s^2$ : outdoor footbridges [9,14]

**Table 6.** Structural model peak accelerations corresponding to two people walking.

Dynamic Loading Models	Tubular Footbridge Peak Accelerations ( $a_p$ in $m/s^2$ )							Limit Accelerations ( $a_{lim}$ in $m/s^2$ )*
	Investigated Sections							
	A	B <sub>1</sub>	B	B <sub>2</sub>	C	D	E	
Load Model I (LM-I)	2.71	0.25	0.97	0.25	0.94	0.81	1.68	0.49
Load Model I (LM-II)	2.93	0.27	1.06	0.27	1.04	0.89	1.84	
Load Model I (LM-III)	2.70	0.26	1.00	0.25	0.97	0.84	1.73	
Load Model I (LM-IV)	2.61	0.31	0.76	0.32	0.75	0.73	1.86	

\* $a_{lim} = 1.5\%g = 0.15 m/s^2$ : indoor footbridges [9,14]

\* $a_{lim} = 5.0\%g = 0.49 m/s^2$ : outdoor footbridges [9,14]

**Table 7.** Structural model peak accelerations corresponding to three people walking.

It must be emphasized that the footbridge overhang sections (Sections A and E, see Figure 16) have presented very high peak accelerations, in all investigated situations, as presented in Tables 5 to 7. This is explained due to the fact that the transient impact produced by the pedestrians on the entrance and exit of the investigated structure have generated high acceleration values.

Based on a quantitative analysis of the maximum accelerations, it was verified that the loading model I (LM-I) has produced the highest peak acceleration values practically in all investigated cases, as illustrated in Tables 5 to 7.

These peak accelerations presented in Tables 5 to 7 are related to a pedestrian normal walking situation. It must be emphasized that the limit acceleration value is equal to  $0.49 \text{ m/s}^2$  [9,14], when the outdoor footbridges are considered in the analysis.

Based on the finite element modelling of the steel-concrete composite tubular footbridge dynamic behaviour, the numerical results presented in Tables 5 to 7 indicated that the dynamic actions produced by human walking led to peak accelerations higher than the limiting values present in design code recommendations (Outdoor footbridges:  $a_{\text{lim}} = 5\%g = 0.49 \text{ m/s}^2$  [9,14]), as depicted in Tables 5 to 7.

## 6. Final remarks

This contribution covers the application of tubular structural elements in pedestrian footbridge design and tries to give an overview about the evaluation of tubular footbridges dynamic behaviour, objectifying to help practical structural engineers to deal with this kind of problem and to allow for a further application of tubular structural elements in pedestrian footbridge design.

The present investigation was carried out based on four dynamic loading models (LM-I to LM-IV) implemented objectifying to incorporate the dynamic effects induced by people walking on the footbridges dynamic response. In these models, the position of the human walking load was changed according to the individual position. However, a more realistic loading model (LM-IV) considered the ascent and descending movement of the human body effective mass at each step load (human walking load) and additionally also incorporates the transient effect due to the human heel impact.

The proposed analysis methodology considered the investigation of the dynamic behaviour, in terms of serviceability limit states, of a composite tubular footbridge, spanning 82.5 m. The structure is composed by three spans (32.5 m, 17.5 m and 20.0 m, respectively) and two overhangs (7.50 m and 5.0 m, respectively). The structural system is constituted by tubular steel sections and a concrete slab and is currently used for pedestrian crossing.

A computational model, based on the finite element method, was developed using the ANSYS program. This model enabled a complete dynamic evaluation of the investigated tubular footbridge especially in terms of human comfort and its associated vibration serviceability limit states.

The results found throughout this investigation have indicated that the dynamic actions produced by human walking could generate peak accelerations that surpass design criteria limits developed for ensuring human comfort. Hence it was detected that this type of structure can reach high vibration levels that can compromise the footbridge user's comfort and especially its safety.

The analysis methodology presented in this paper is completely general and is the author's intention to use this solution strategy on other pedestrian foot-bridge types and to investigate the fatigue problem. The fatigue problem is a relevant issue and certainly much more complicated and is influenced by several design parameters and footbridge types. Further research in this area is currently being carried out.

### Author details

José Guilherme Santos da Silva, Ana Cristina Castro Fontenla Sieira, Gilvan Lunz Debona, Pedro Colmar Gonçalves da Silva Vellasco and Luciano Rodrigues Ornelas de Lima  
*State University of Rio de Janeiro (UERJ), Rio de Janeiro/RJ, Brazil*

### Acknowledgement

The authors gratefully acknowledge the support for this work provided by the Brazilian Science Foundation CAPES, CNPq and FAPERJ.

### 7. References

- [1] Debona GL. Modelagem do comportamento dinâmico de passarelas tubulares em aço e mistas (aço-concreto) (Modelling of the dynamic behaviour of steel-concrete composite tubular footbridges), MSc Dissertation (in Portuguese), Civil Engineering Post-Graduate Programme, PGECIV, State University of Rio de Janeiro, UERJ, Rio de Janeiro, Brazil, pp. 1-154; 2011.
- [2] Zúñiga JEV. Análise da resposta dinâmica experimental de uma passarela tubular mista, aço-concreto, submetida ao caminhar humano (Dynamic experimental analysis of a steel-concrete composite tubular footbridge submitted to human walking), MSc Dissertation (in Portuguese), Civil Engineering Post-Graduate Programme, PGECIV, State University of Rio de Janeiro, UERJ, Rio de Janeiro, Brazil, pp. 1-135; 2011.
- [3] Figueiredo FP, Silva JGS da, Vellasco PCG da S, Andrade SAL de, Andrade, SAL de. A parametric study of composite footbridges under pedestrian walking loads. *Engineering Structures*, 2008; 30:605-615.
- [4] Silva JGS da, Vellasco PCG da S, Andrade SAL de, Lima LRO de, Figueiredo FP. Vibration analysis of footbridges due to vertical human loads. *Computers & Structures*, 2007; 85:1693-1703.
- [5] Eurocode 3: Design of steel structures. Part 1.9: General rule - Fatigue. European Committee for Standardisation; 2005.

- [6] Kuhlmann U, H-P Günther, Saul R, Häderle, M.-U. 2003. Welded circular hollow section (CHS) joints in bridges. ISTS 2003: Proceedings of the 10th International Symposium on Tubular Structures, Madrid, Spain.
- [7] Leitão FN, Silva JGS da, Vellasco PCG da S, Lima LRO de, Andrade SAL de. Composite (steel-concrete) highway fatigue assessment. *Journal of Constructional Steel Research*, 2011; 67(1):14-24.
- [8] Varela WD. Modelo teórico-experimental para análises de vibrações induzidas por pessoas caminhando sobre lajes de edifícios (Theoretical-experimental model to analyse vibrations induced by people walking on floor slabs of buildings), PhD Thesis (in Portuguese), Federal University of Rio de Janeiro, Civil Engineering Department, COPPE/UFRJ, Rio de Janeiro, Brazil, pp. 1-309; 2004.
- [9] Murray TM, Allen DE, Ungar EE. Floor vibrations due to human activity, *Steel Design Guide Series*, American Institute of Steel Construction, AISC, Chicago, USA; 2003.
- [10] Pimentel RL, Pavic A, Waldron, P. Evaluation of design requirements for footbridges excited by vertical forces from walking. *Canadian Journal of Civil Engineering*, 2001; 28(5),769-776.
- [11] Chen, Y. Finite element analysis for walking vibration problems for composite precast building floors using ADINA: modelling, simulation and comparison. *Computer & Structures*, 1999; 72:109-126.
- [12] Bachmann, H, Ammann, W. Vibrations in structures induced by man and machines, *Structural Engineering Document 3e*. International Association for Bridges and Structural Engineering; 1987.
- [13] ANSYS. Swanson Analysis Systems, Inc. P.O. Box 65, Johnson Road, Houston, PA, 15342-0065, Version 10.0, Basic analysis procedures, Second edition; 2003.
- [14] International Standard Organization / ISO 2631-2. Evaluation of human exposure to whole-body vibration, Part 2: Human Exposure to Continuous and Shock-Induced Vibrations in Buildings (1 to 80Hz), International Standard; 1989.
- [15] Comité Euro-international du Béton. CEB-FIP: Bulletin d'information, N<sup>o</sup> 209, England, London, August; 1993.